

United States Department of Agriculture



Natural Resources Conservation Service  
National Soil Survey Center  
Federal Building, Room 152  
100 Centennial Mall North  
Lincoln, NE 68508-3866

Phone: (402) 437-5499  
FAX: (402) 437-5336

SUBJECT: SOI – Geophysical Assistance

June 20, 2013

TO: Dr. Henry Lin  
Professor of Hydropedology/Soil Hydrology  
Department of Ecosystem Science and Management  
415 Agricultural Sciences and Industries Building  
Pennsylvania State University  
University Park, Pennsylvania 16802

File Code: 330-7

Denise Coleman  
State Conservationist  
NRCS, Harrisburg, Pennsylvania

**Purpose:**

Geophysical investigations were conducted at the Shale Hills *Critical Zone Observatory (CZO)* in Huntingdon County, and at the Pennsylvania State University's *Living Filter Field* in Centre County, Pennsylvania. The Shale Hills CZO serves as an experimental catchment for the study of spatial and temporal variations in hydrological response. The focus of the present research at Shale Hills CZO is to characterize the depth to rock, stratigraphic layers and soil horizons that influence the flow of water through different soil-landscape components within the catchment. At the *Living Filter Field*, electromagnetic induction (EMI) is used to characterize spatial-temporal changes in soil properties that influence apparent conductivity.

**Participants:**

Jim Doolittle, Research Soil Scientist, NSSC, NRCS, Newtown Square, PA  
Isaac Hopkins, MS Student, Department of Ecosystem Science and Management, Pennsylvania State University, University Park, PA  
Liu Hu, Post-Doctorate, Department of Ecosystem Science and Management, Pennsylvania State University, University Park, PA  
Henry Lin, Professor of Hydropedology/Soil Hydrology, Department of Ecosystem Science and Management, Pennsylvania State University, University Park, PA  
Haolinag Yu, Ph.D. student, Department of Ecosystem Science and Management, Pennsylvania State University, University Park, PA

**Activities:**

Field activities were completed during the period of April 30-May 2, 2013.

**Summary:**

1. Ground-penetrating radar was used to determine the depth and characterize the spatial structural variability of the underlying rock within the Shale Hills CZO. Within the Shale Hills CZO, soils



are dominantly shallow (Weikert series) and moderately deep (Berks series) to rock. Soils are shallower on higher-lying soil-landscape components and moderately deep and deeper soils on lower-lying soil-landscape components.

2. Within an investigated swale, soils are shallow and moderately deep to rock on exterior, convex and linear shoulder and back slope components. Soils are mostly very deep to rock on interior, concave foot and toe slopes. Soils are deep to rock on some concave back and foot slopes, but this depth class is a minor component within this swale.
3. For the eight radar traverses conducted across and along the swale, the average depth to rock is 1.22 m with a range of 0.12 to 3.46. Beneath the traversed portions of the swale, the depth to rock is 36% shallow, 22% moderately deep, 11% deep, and 30% very deep.
4. Based on 193,893 georeferenced radar depth measurements obtained in several studies conducted over the years, soils are 62% shallow, 20% moderately deep, 9% deep, and 9% very deep within the Shale Hills watershed.
5. Electromagnetic induction was used to survey portions of the *Living Filter Field*. Returning to this site at a drier time of the year should provide comparative information on spatiotemporal variations in soil moisture.
6. The results of this study are interpretative. Geophysical interpretations are considered preliminary estimates of site conditions. The results of geophysical site investigations do not substitute for direct observations, but rather reduce their number, direct their placement, and supplement their interpretations. Interpretations contained in this report should be verified by ground-truth observations.



DAVID R. HOOVER  
Acting Director  
National Soil Survey Center

ACTING

cc:

Joseph Kraft, State Soil Scientist, NRCS, Harrisburg, PA  
Robert Dobos, Soil Scientist & Liaison for MO6, NSSC, MS 36, NRCS, Lincoln, NE  
Jim Doolittle, Research Soil Scientist, NSSC, NRCS, Newtown Square, PA  
David Kingsbury, Soil Survey Regional Director, NRCS, Morgantown, WV  
J. Cameron Loerch, Acting National Leader, Soil Survey Research & Laboratory, NSSC, MS 41, NRCS, Lincoln, NE  
David W. Smith, Director, Soil Science Division, NRCS, Washington, DC  
Wes Tuttle, Soil Scientist (Geophysical), NSSC, NRCS, Wilkesboro, NC

**Technical Report on Geophysical Investigations conducted at the Shale Hills *Critical Zone Observatory* and at Pennsylvania State University's *Living Filter Field* on April 30-May 2, 2013.**

**James A. Doolittle**

**Shale Hills Watershed:**

The Shale Hills Watershed and Critical Zone Observatory (CZO) is located in northern Huntingdon County. The watershed is in the *Ridge and Valley Province* of central Pennsylvania. This relatively small (0.08 km<sup>2</sup>), forested watershed is defined by two merging ridge lines (Figure 1). These ridge lines are truncated to the west by a relict stream terrace through which Shaver Creek presently flows. Within the watershed, elevations range from about 256 to 310 m. Slopes are gently sloping to steep. The watershed is underlain by the Silurian Rose Hill formation. This formation consists of thinly bedded, steeply inclined shale strata. An oak-hickory forest dominates most of the watershed. However, a less extensive oak-hemlock community exists along the lower reaches of the stream that drains the watershed.

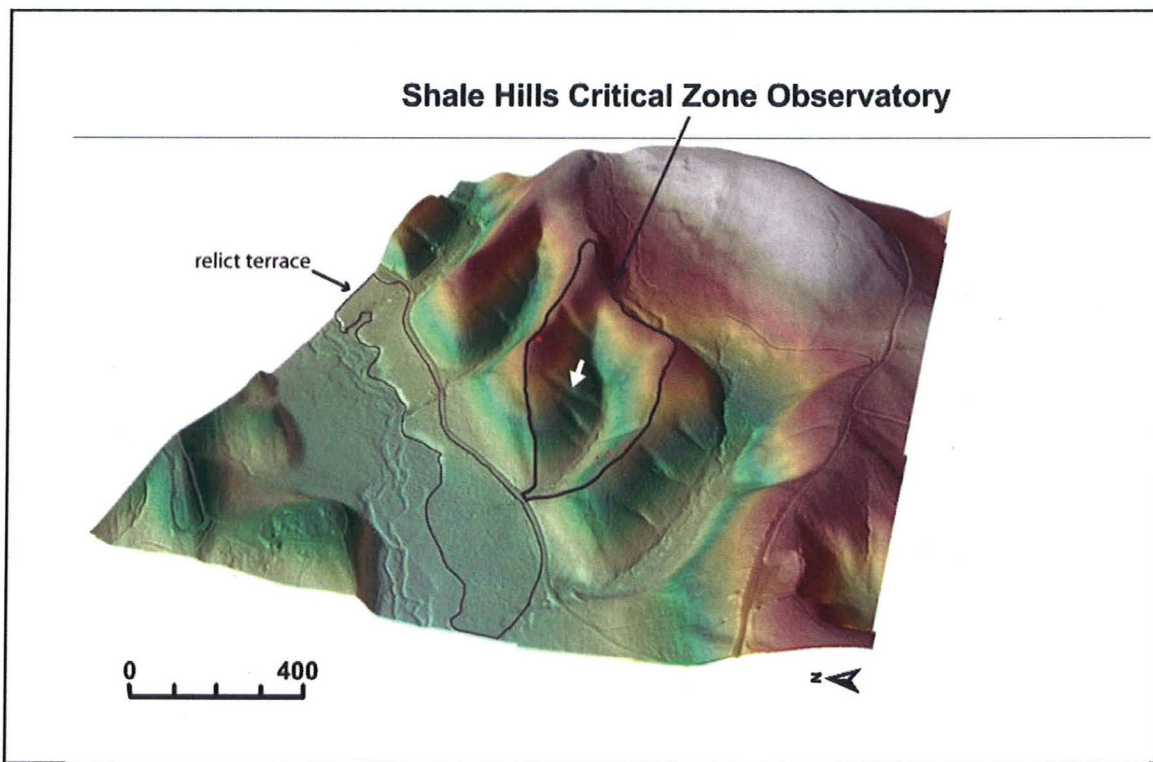


**Figure 1. This digital elevation model is constructed from LIDAR data and shows the location of the Shale Hills CZO and the topography of the surrounding area.<sup>1</sup>**

The Soil Survey Report for Huntingdon County (Merkel, 1978) has the watershed mapped mostly as Berks-Weikert soils, steep; and Ernest channery silt loam, 3 to 8 percent slopes. The watershed also includes small areas of Berks-Weikert shaly silt loam, 15 to 25 percent slopes; and Berks shaly silt loam, 8 to 15 percent slopes. These shallow to very deep soils formed in materials weathered from shale. The results of a more recent, high intensity soil survey of the watershed are shown in Figure 2. The well

<sup>1</sup> Geomorphic map of Shale Hills CZO is from <http://criticalzone.org/shale-hills/infrastructure/gis-remote-sensing-geophysics-shale-hills/>. Accessed on 6/6/2013.

drained, shallow (25 to 50 cm) Weikert soils dominate linear and convex summit, shoulder and back slope positions. The moderately deep (50-100 cm) Berks soils are on slightly concave and linear slopes and drainage heads. The high-intensity survey also reveals areas of very deep (> 150 cm), excessively drained Rushtown soils in narrow gullies (henceforth referred to as *swales*) that descend the back slopes of the watershed to the stream terrace. The swales have been sculpted by running water cutting through the rock on the steeply sloping back slopes of the ridges that define the watershed. A narrow terrace borders the stream that flows from the watershed. On this terrace, the very deep, moderately well drained Ernest, and the moderately deep, somewhat poorly drained and moderately well drained Blairton soils are mapped (Figure 2). Ernest soil has a fragipan within depths of about 50 to 90 cm. All of the aforementioned soils contain large amounts of rock fragments and are underlain by thinly bedded and highly fractured shale. Table 1 lists the taxonomic classification of these soils.

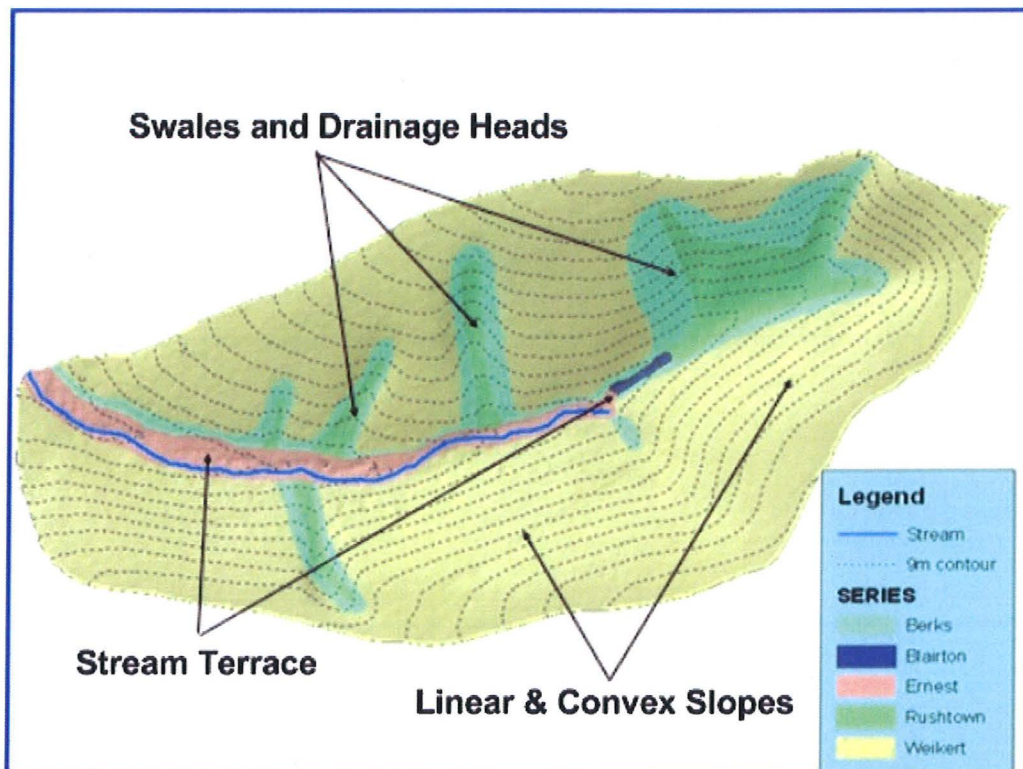


Figure 2. A high intensity soil map of the Shale Hills watershed shows the distribution of soils on different landscape components. The arrow is believed to indicate the swale surveyed during this investigation.

Table 1. Taxonomic classification of soils.

Series	Taxonomic Classification
Berks	loamy-skeletal, mixed, active, mesic Typic Dystrudepts
Blairton	fine-loamy, mixed, active, mesic Aquic Hapludults
Ernest	fine-loamy, mixed, superactive, mesic Aquic Fragiudults
Rushtown	loamy-skeletal over fragmental, mixed, active, mesic Typic Dystrudepts
Weikert	loamy-skeletal, mixed, active, mesic Lithic Dystrudepts

The focuses of this study is a south-facing swale (identified by arrow in Figure 1). The objective of this study is to characterize the depth to rock within this swale and to summarize the depth to rock data that have been recorded using GPR and GPS within the watershed.

## **GPR**

### **Equipment:**

The radar unit is the TerraSIRch Subsurface Interface Radar (SIR) System-3000 (SIR-3000), manufactured by Geophysical Survey Systems, Inc. (GSSI; Salem, NH).<sup>2</sup> The SIR-3000 consists of a digital control unit (DC-3000) with keypad, SVGA video screen, and connector panel. A 10.8-volt lithium-ion rechargeable battery powers the system. The SIR-3000 weighs about 9 lbs (4.1 kg) and is backpack portable. With an antenna, the SIR-3000 requires two people to operate. Daniels (2004) and Jol (2008) discuss the use and operation of GPR. A 200 MHz antenna with survey wheel was used to record soil depths within the swale. A 400 MHz antenna was used in previous investigations to document soil depths on back slope and summit areas (where the depth to rock was shallower).

The RADAN for Windows (version 7.0) software program (developed by GSSI) was used to process the radar records shown in this report.<sup>2</sup> Processing included: header editing, setting the initial pulse to time zero, color table and transformation selection, signal stacking, horizontal high-pass filtration, range gain adjustments and surface normalization (refer to Jol (2009) and Daniels (2004) for discussions of these techniques). The *Interactive 3D Module* of RADAN was used to semi-automatically “pick” the depths to the interpreted soil/rock interface on radar records. The picked data were exported to a worksheet (in an X, Y, and Z format; including longitude, latitude, and depth to rock) for documentation.

The SIR-3000 system contains a setup for the use of a GPS receiver with a serial data recorder. With this setup, each scan of the radar can be geo-referenced (position/time matched). Following data collection, a subprogram within the RADAN for Windows software program is used to proportionally adjust the position of each radar scan according to the time stamp of the two nearest positions recorded with the GPS receiver. A Trimble AG114 L-band DGPS (differential GPS) antenna (Trimble, Sunnyvale, CA) was used to collect position data.<sup>2</sup> Position data are recorded at a rate of one reading per second.

### **Calibration of GPR:**

Ground-penetrating radar is a time scaled system. The system measures the time that it takes electromagnetic energy to travel from an antenna to an interface (e.g., rock, soil horizon, stratigraphic layer) and back. To convert the travel time into a depth scale, either the velocity of pulse propagation or the depth to a reflector must be known. The relationships among depth (D), two-way pulse travel time (T), and velocity of propagation (v) are described in equation [1] (after Daniels, 2004):

$$v = 2D/T \quad [1]$$

The velocity of propagation is principally affected by the relative dielectric permittivity ( $E_r$ ) of the profiled material(s) according to equation [2] (after Daniels, 2004):

$$E_r = (C/v)^2 \quad [2]$$

In equation [2], C is the velocity of propagation in a vacuum (0.3 m/ns). Typically, velocity is expressed in meters per nanosecond (m/ns). In soils, the amount and physical state (temperature dependent) of water have the greatest effect on the  $E_r$  and v. At the time of this studies, soils were moist.

Based on the measured depth and the two-way pulse travel time to a known subsurface reflector (metal plate buried at 50 cm), the v and  $E_r$  through the upper part of a Rushtown soil profile were estimated using equations [1] and [2]. For the 200 MHz antenna, the estimated v was 0.0882 m/ns and the estimated  $E_r$  was 11.62. These values were used to convert the time-scale into a depth scale on the radar records that were collected during this study.

---

<sup>2</sup> Manufacturer's names are provided for specific information; use does not constitute endorsement.

**Field Methods:**

Multiple GPR traverses are completed by pulling the 200 MHz antenna along the ground surface. A distance-calibrated survey wheel with encoder was bolted onto the antenna and provided greater controls over signal pulse transmission and data collection. The survey wheel experienced some slippage, which did result in some recorded line lengths (from the survey wheel) being slightly different from the actual lengths. Each radar traverse was stored as a separate file. The GPS option was used with the SIR-3000 system, and a majority of the radar scans were reasonably and accurately geo-referenced. The Trimble AgGPS receiver was operated in the autonomous (GPS only) mode with a described horizontal accuracy of approximately 3–9 meters. However, multipath distortion and satellite shading (caused by slope and vegetation obstructions), lessened the positional accuracy and reduced the number of radar traverses and scans that could be satisfactorily geo-referenced with GPS. Other sources of positioning error included the number of satellites in view, satellite geometry, ionospheric conditions, and of course, the quality of GPS receiver. In order to *surface normalize* the radar records, relative elevation data were collected at major breaks in the slope along each traverse line with an engineering level and stadia rod.

**Results:**

Eight radar traverses were completed across a south-facing swale within the Shale Hills CZO (see Figure 1 for approximate location) using a 200 MHz antenna. With the exception of the lowermost traverse line (line 1), the approximate locations of these lines within the swale are shown in Figure 3. For traverse line 1, the identity of a major subsurface interface, evident on the radar record, was unclear and did not correspond with the depths to rock observed in cores that had been previously extracted nearby. As a consequence, this line has not been shown on Figure 3. In Figure 3, colors have been used to identify the different soil depth classes (white - shallow; red - moderately deep; yellow – deep; and green (150 to 200 cm) and blue (> 200 cm) – very deep) along each traverse line.

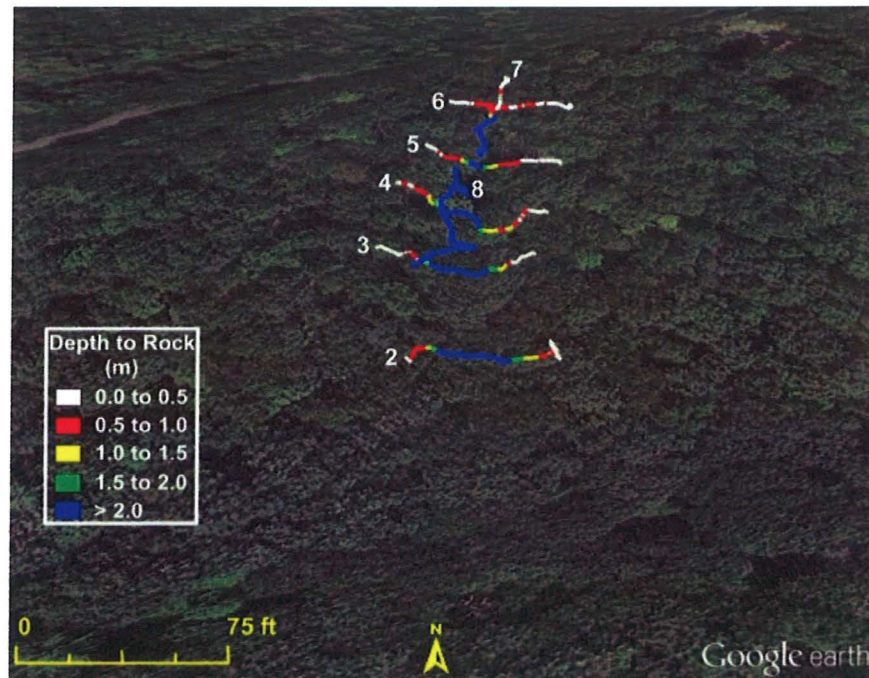


**Figure 3. This Google Earth image shows the approximate locations of the GPR traverses completed on a south-facing swale in the Shale Hills CZO. The depth to rock is indicated by the color-codes used along each of the traverse lines.**

Six of the traverse lines (#1 to #6) were conducted normal to the long axis of the swale from west to east. These traverses began and ended near conspicuous breaks in the slope, which defined the peripheral boundaries of the swale. Two traverses (#7 and #8) were conducted downslope along the center line of the swale. As evident in Figure 3, segments of several traverse lines were poorly positioned with GPS.

The dominant slope shape within the swale is concave, both orthogonal and parallel with the contours. Soils are shallow and moderately deep to rock on the swale’s exterior, convex and linear shoulder and back slope components (Figure 3). Soils are mostly very deep to rock on the swale’s interior, concave foot and toe slopes. Soils are deep (100 to 150 cm) to rock on some concave back and foot slopes, but this depth class is a minor component within this swale. Table 2 summarizes the range and average depth to rock along each of the six traverse lines.

**Table 2. Basic Statistics on the depth to rock along GPR traverses that crossed the swale. All depths are in meters.**

Traverse	Average	Minimum	Maximum
1	0.67	0.22	1.11
2	1.32	0.24	3.29
3	1.16	0.15	3.02
4	1.18	0.26	3.03
5	1.07	0.22	2.73
6	0.40	0.15	0.79

As evident in Figure 3, the depth to rock deepens toward the interior and center line of the swale. Traverse line 6 is located at the head of the swale where the slope shape is dominantly convex (down slope) concave (across slope). Relative relief along this line is about 1.52 meters. Compared with data from the other traverse lines, soil depths are relatively shallow and less variable along traverse line 6 (see Table 2).

As evident in Figure 3, the swale deepens and widens in a downslope direction between traverse lines 5 to 2. Within this portion of the swale, the relative relief along the traverse lines ranges from about 2.1 to 4.4 meters (along lines 2 and 4, respectively). Although the relief is greatest along traverse lines 4 and 3 (4.0 m), the swale is widest along traverse line 2. Along traverse line 2, the layers of colluvium are thickest (Table 2) and the extent of very deep soils is the most expansive (Figure 3).

Traverse line 1 (not shown in Figure 3) is located at the base of the swale where this feature merges with the stream terrace. Here the slopes are dominantly concave (down slope) linear (across slope) and relatively subdued. The interpretation of a major subsurface interface and the depth to rock were unclear on the radar record from this traverse line.

The radar records that were obtained within the swale were generally of good interpretive quality and the soil/rock interface was, in general, confidently identified. In places, the soil/rock interface appeared highly segmented and variable in depth on the radar records. Where these conditions occurred, and if there were multiple reflections in the overlying soil materials, the identification of the soil/rock interface was more challenging and interpretations more uncertain. As in previous studies, the shale was virtually free of internal radar reflectors. The shale forms a zone of “no radar returns,” which contrasts strongly with the multiple radar reflections apparent in the overlying soil. The lack of internal reflectors, however, aided the identification of the shale. Bands of unwanted, low frequency noise were present in the lower parts of the radar records. These bands of noise were easily identified as they are broader than radar

reflections, look sullied, and parallel the soil surface. A majority of these bands were removed from the radar records using horizontal high-pass filtration processing.

Surface normalization procedures were used to correct the reflection patterns on radar records for changes in elevation. This processing technique greatly aids interpretations and the association of subsurface reflectors with soils and landscape components. Figures 4 and 5 contain surface normalized radar records of the six traverse lines that were completed orthogonal to the long axis of the swale. On each of these surface-normalized radar records, a red-colored, segmented line has been used to highlight the interpreted soil/rock interface. On these radar records, all scales are expressed in meters.

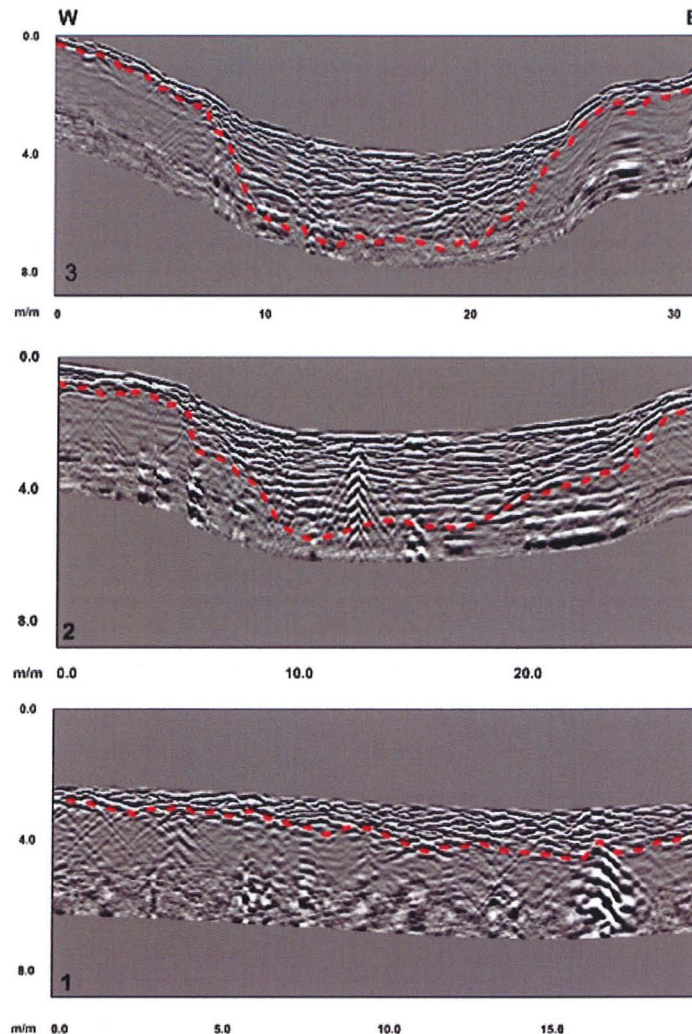


**Figure 4. These three radar traverses were conducted orthogonal to the long axis of the swale. The traverses form an orderly sequence upwards from the swale's base (1) to near its midsection (3) (see Figure 3 for the locations of lines 2 and 3). All measurements are expressed in meters.**

As evident in Figure 4, the topographic form of a swale is not evident along traverse line 1 (lowermost radar record), which is the closest line to the stream terrace. Along this traverse line, the deepest recognizable interface has been tentatively identified as the soil/rock boundary. Below this interface, other than low-frequency background noise, reflections are generally weakly expressed or absent. In other parts of the watershed, this zone of “no signal return” has been interpreted as the shale. However,

core data in the general vicinity of this traverse reveal deeper depths to rock. Lacking ground truth verification, the present interpretation is troubling and highly suspect.

Moving up the swale to traverse line 2 (Figure 4, middle radar record), a noticeable surface concavity appears. The trough beneath this topographic concavity is filled with planar reflectors, which are believed to represent strata of contrasting grain-size, density and/or moisture contents. The colluvium that fills the swale is noticeably deeper and better expressed along traverse line 2 than the deposits shown along line 1. Along line 2, the strongly expressed reflection hyperbola near 14 m (horizontal scale) was produced by a utility cable that extends upslope within the swale.

Along traverse line 3 (Figure 4, uppermost radar record) the slopes that form the topographic concavity are steeper than along traverse lines 1 and 2. As evident along both traverse lines 2 and 3, soils rapidly deepen and transition from shallow to very deep as one descends into the swale. On line 3, the trough is filled with both horizontal and inclined planar reflectors. Compared with the structure displayed along traverse line 2, along traverse line 4, the swale is similar in depth, but is narrower and has steeper side slopes.

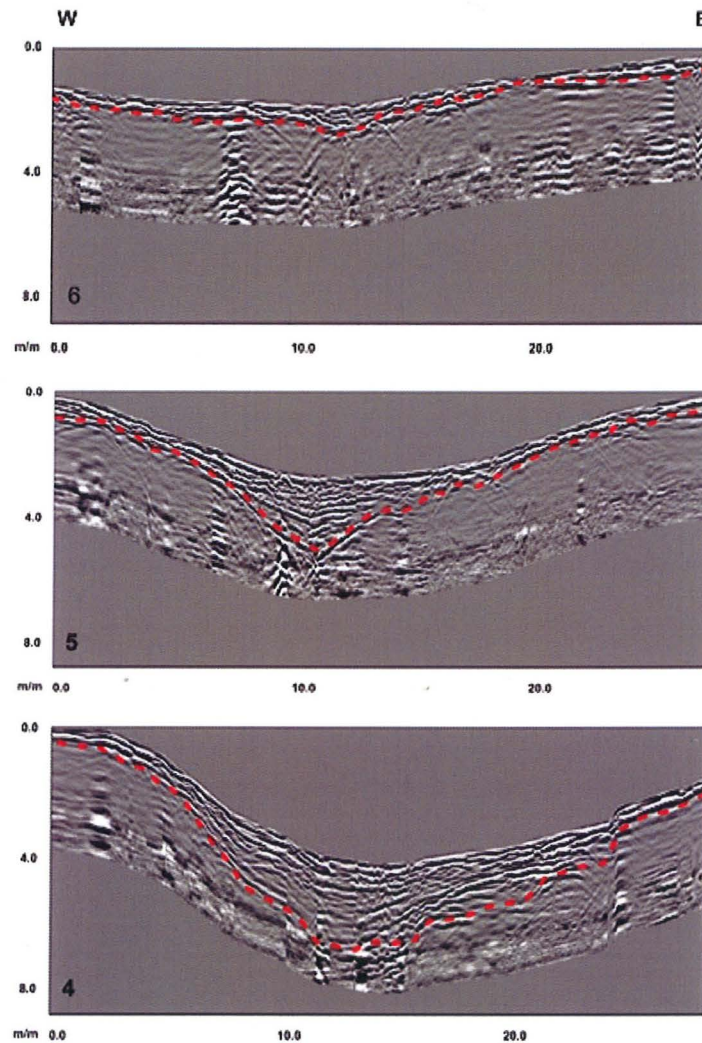


**Figure 5. These three radar traverses were conducted orthogonal to the long axis of the swale. The traverses form an orderly sequence upwards from near the swale's midsection (4) to near its apex (6) (see Figure 3 for the locations of these lines). All measurements are expressed in meters.**

Figure 5 contains three radar traverses that span the swale from near its mid-section to near its apex. Compared with the other traverse lines that were completed across the swale, along traverse line 4, relief and slope asymmetry achieve their greatest expression. Along traverse lines 4 and 5, the deepest portion of the swale has shifted toward the western side and slightly away from centerline of the swale. The thickness and mass of colluvium within the swale becomes less as one continues to ascend the centerline of the swale from traverse lines 4 to 6.

In each of the radar records shown in Figure 5, the strongly expressed reflection hyperbola that appears to the left (west) of the swale's centerline represents the reflections and reflection multiples from a buried utility line. Along traverse lines 4 and 5, contrasting layers of colluvium produce horizontal and inclined planar reflectors within the swale. Along traverse line 6, which is located near the apex of the swale, layers of colluvium are very thin or not present. As evident on the radar records shown in Figures 4 and 5, the swale has an asymmetrical cross section with its western slopes being higher than its eastern slopes. This asymmetry is evident in traverse lines 1 thru 5.

The quality of the two radar traverses that were conducted downslope along the centerline of the swale was poor. Although the depths to rock could be interpreted along these traverses, the imagery was broken into segments that were difficult to image. Figure 6 is a reconstruction of radar record from traverse line 7, which originates close to the swale's head and descends the swales near its centerline. In Figure 6, the two high-amplitude reflection hyperbolas and their reverberations were produced by the antenna passing over the same utility line. For the first 14 meters of this traverse line the soil is shallow and moderately deep to rock. Between the 14 and 16 meter distance mark, the depth to rock deepens and is very deep for the remainder of the traverse. The colluvium that overlies the rock appears highly stratified.

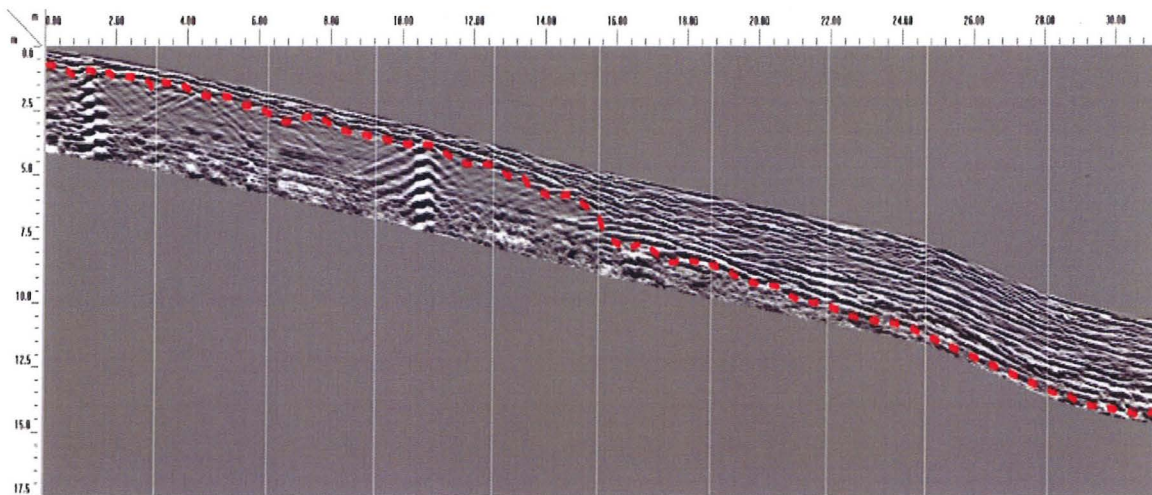


**Figure 6. This surface normalized radar record was taken along a traverse line that followed the centerline of the swale from its apex to a point 31 meters downslope. All measurements are expressed in meters. The segmented red-colored line identifies the interpreted soil/rock interface.**

For the eight radar traverses conducted across and along the swale, a total of 12,920 geo-referenced radar measurements were obtained on the depth to rock. Along these traverse lines, the average depth to rock is 1.22 m with a range of 0.12 to 3.46. Table 3 groups the data collected along these traverse lines into the standard soil depth classes. Beneath the traversed portions of the swale, the depth to rock is 36% shallow, 2% moderately deep, 11% deep, and 30% very deep. A bar graph showing the distribution of the 12,920 soil-depth measurements is presented in Figure 7. This distribution is skewed to the right. This non-

symmetrical distribution suggests the complexity of estimating a "typical value" for the depth to rock within the swale.

**Table 3. The number and frequency of measurements are grouped into soil depth classes for the GPR traverses that were conducted on a south-facing swale.**

Depth Class (cm)	Number	Frequency
< 50	4662	0.36
50 to 100	2866	0.22
100 to 150	1466	0.11
150 to 200	1194	0.09
>200	2732	0.21

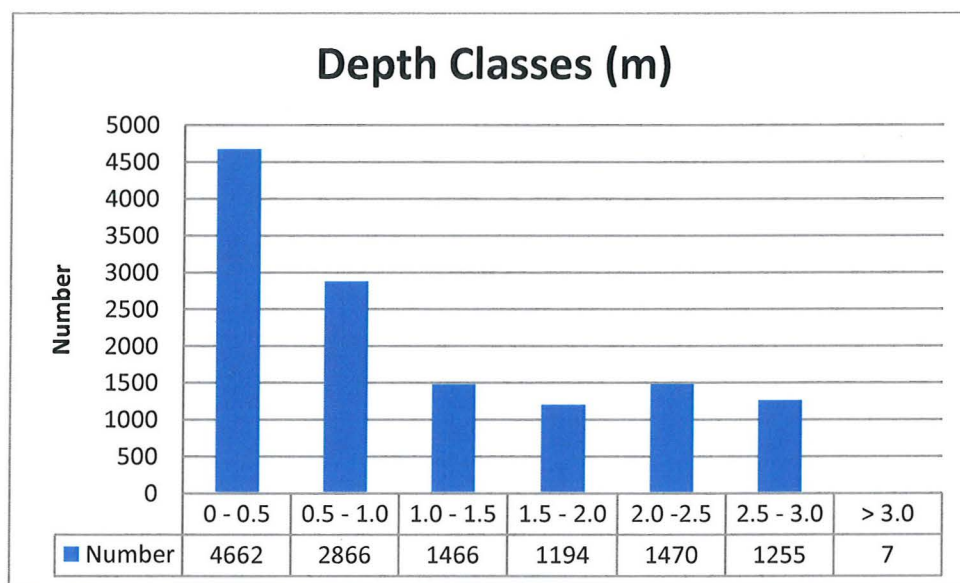


**Figure 7. This bar graph shows the distribution of soil-depth measurements obtained with GPR on a south-facing swale. The depth intervals are expressed in meters.**

Summary of all Georeferenced GPR traverses in the Shale Hills Watershed:

Figure 8 is a Google Earth image showing the location of all georeferenced GPR traverses that have been completed across the Shale Hills watershed. Colors have been used to identify the different soil depth classes. As evident in Figure 8, soils are dominantly shallow along the trail that encircles the watershed and delineates its perimeter and summit area. Along these higher-lying radar traverse lines, the average depth to rock is 31 cm with a range of 0 to 79 cm. Soils are 96% shallow and 4% moderately deep along these summit traverse lines. Soils are deeper on lower slope components within the interior of the watershed. Along these lower-lying radar traverse lines, the average depth to rock is 59 cm with a range of 10 to 161 cm. Soils are 43% shallow, 50% moderately deep and 7% deep along these lower-lying, more interior traverse lines.

Based on 193,893 georeferenced radar depth measurements, soils along the selected traverse lines shown in Figure 8 are 62% shallow, 20% moderately deep, 9% deep, and 9% very deep. The GPR data conflict with the generalized soil map of the watershed, which depicts a dominance of Berks (moderately deep) and Ernest (very deep) soils. However, even the distribution of soil depths interpreted with GPR does not

convey an accurate impression of their spatial variability across the various landscape components within the watershed.

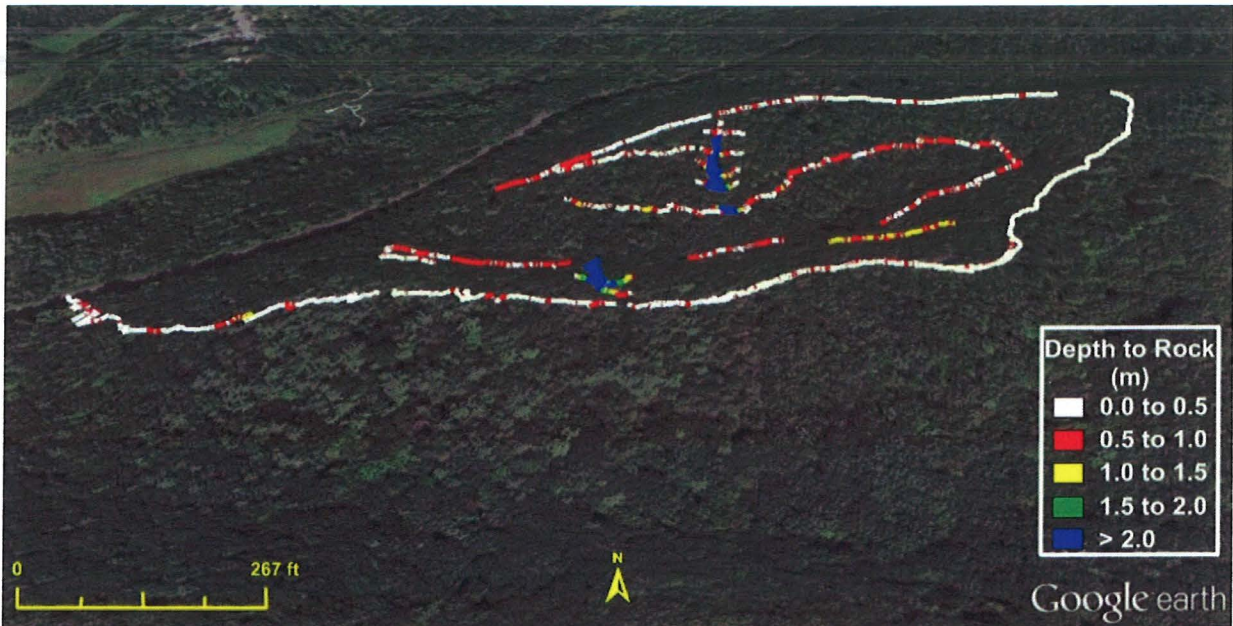


**Figure 8. This Google Earth image of the Shale Hills CZO shows a composite of the collected geo-referenced GPR traverse data.**

Wide differences in the depth to rock can be observed on different landscape components in the Shale Hills watershed. As evident in Figure 6, shallow Weikert soils dominate the watershed. Shallow soils are especially dominant on higher-lying slope components and the summit areas that rim the watershed. Deeper soils are more extensive on lower-lying slope components and in swales.

Figure 9 contains three bar graphs showing the distribution of soil depths on different landscape components and landforms. On convex summit, shoulder, and upper back slopes (upper bar graph in Figure 9), soils are 82% shallow and 16% moderately deep to rock. Deep and very deep soils comprise only 2% of the acreage on these landscape components. On lower-lying linear and concave back slopes (middle bar graph in Figure 9), soil depths are more uniformly distributed with 27% shallow, 37% moderately deep, and 35% deep soils. However, for traverses conducted across swales (lower bar graph in Figure 9); soils are 51% shallow, 16% moderately deep, 6% deep, and 26% very deep. The dominance of shallow soils in swales is at first surprising. However, the radar traverses that were conducted orthogonally to the long axis of the swale typically included substantial areas on Weikert soils on the higher-lying, more steeply sloping, upper back and shoulders slopes that descend into the swales. In addition these traverse lines often extended beyond the limits of the swales.

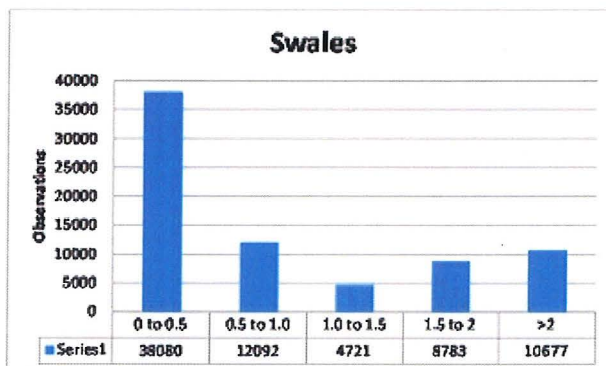
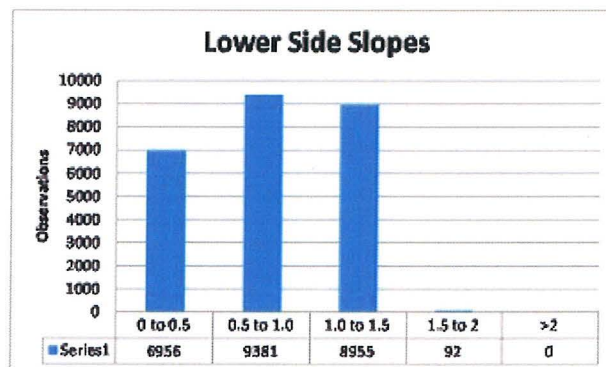
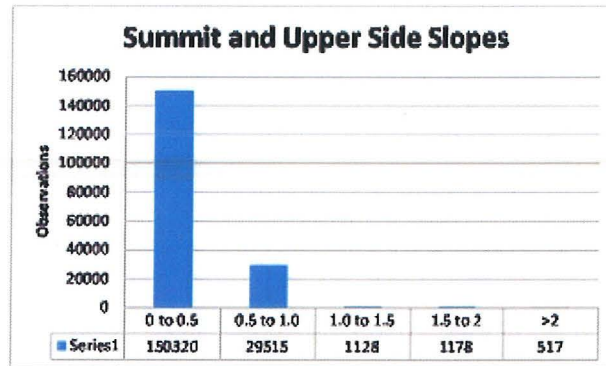


**Figure 9.** These bar graphs show the distribution of soil-depth measurements obtained with GPR on different slope positions and landforms. The five depth intervals are expressed in meters.

**EMI:**

*Living Filter Field:*

Electromagnetic induction surveys were completed across a portion of the Pennsylvania State University's *Living Filter Field*. The Living Filter Research Project sprays sewage effluent onto wood land and agricultural plots as part of a wastewater renovation cycle in which the biologically active soil serves as the final treatment step in sewage effluent remediation. The *Living Filter Field* has been in continuous operation since 1982. The field receives as much as 2 inches of sprayed effluent per week.



**Figure 10 - This soil map shows the areas that are surveyed (enclosed by segmented lines) at the Living Filter Field.**

The EMI survey was confined to the southern, cultivated portion of the *Living Filter Field*. Figure 10 is a soil map of the portion of the *Living Filter Field* that was surveyed.<sup>3</sup> This area has been mapped as Hagerstown silt loam, on 3 to 8 percent slopes (HaB) and 8 to 15 percent slopes (HaC). The deep and very deep, well drained Hagerstown soils formed in residuum weathered from limestone. Hagerstown is a member of the fine, mixed, semiactive, mesic Typic Hapludalfs taxonomic family.

#### **EMI Meters:**

The EM38-MK2 meter (Geonics Limited; Mississauga, Ontario) was used in this study.<sup>4</sup> Operating procedures for the EM38-MK2 meter are described by Geonics Limited (2007). The EM38-MK2 meter operates at a frequency of 14.5 kHz and weighs about 5.4 kg (11.9 lbs.). The meter has one transmitter coil and two receiver coils, which are separated from the transmitter coil at distances of 1.0 and 0.5 m. This configuration provides two nominal exploration depths of 1.5 and 0.75 m when the meter is held in the vertical dipole orientation (VDO), and 0.75 and 0.38 m when the meter is held in the horizontal dipole orientation (HDO). The EM38-MK2 provides simultaneous measurement of both the quadrature phase (apparent conductivity) and in-phase (apparent magnetic susceptibility) components, each within two distinct depth ranges, without any requirement for soil-to-instrument contact.

The Geonics DAS70 Data Acquisition System was used with the EM38-MK2 meter to record and store both EMI and GPS data. The acquisition system consists of the EMI meter, an Allegro CX field computer (Juniper Systems, Logan, Utah), and a Trimble Ag114 L-band DGPS (differential GPS)

<sup>3</sup> Soil Survey Staff, Natural Resources Conservation Service, United States Department of Agriculture. Web Soil Survey. Available online at <http://websoilsurvey.nrcs.usda.gov/> accessed [06/4/2013].

<sup>4</sup> Manufacturer's names are provided for specific information; use does not constitute endorsement.

antenna (Trimble, Sunnyvale, CA).<sup>4</sup> With the acquisition system, the meter is keypad operated and measurements are automatically triggered. The RTmap38MK2 software program developed by Geomar Software Inc. (Mississauga, Ontario) was used with the EM38-MK2 meter and the Allegro CX field computer to record, store, and process EC<sub>a</sub> and GPS data.<sup>4</sup>

To help summarize the results of the EMI surveys, SURFER for Windows (version 10.0), developed by Golden Software, Inc. (Golden, CO), was used to construct the simulations shown in this report.<sup>4</sup> Grids of EC<sub>a</sub> data were created using kriging methods with an octant search.

**Field Procedures:**

The EM38-MK2 meter was operated in the deeper-sensing VDO, and in the continuous recording mode with measurements recorded at a rate of 1/sec. The meter was placed in a plastic sled with its long axis orientated parallel to the direction of traverse. The sled was towed behind a 4WD all-terrain-vehicle (ATV). By driving the ATV in a back and forth manner across the site along essentially parallel traverse lines, a total of 4302 measurements were recorded with the EM38-MK2 meter. Above ground irrigation pipes were given a wide berth and not approached with the ATV and sled. At the time of the EMI surveys, soils were moist throughout. At the meter’s calibration site, the recorded soil temperature was 52° F at a depth of 50 cm. All EC<sub>a</sub> data were corrected to a standard temperature of 75° F.

**Results:**

EMI:

Basic statistics for the EMI survey are listed in Table 4. For the data collected with the 100-cm intercoil spacing (exploration depth of 150-cm), EC<sub>a</sub> averaged 30.1 mS/m and ranged from -4.0 to 56.3 mS/m. This average EC<sub>a</sub> and the interquartile range (28 to 32 mS/m) are considered representative of Hagerstown soils. Negative values are associated with metallic artifacts scattered or buried across the site. The distribution of these measurements is graphed in Figure 11. As evident in this bar graph, EC<sub>a</sub> measurements obtained with the 100-cm intercoil spacing are concentrated about 30 and 40 mS/m.

**Table 4. Basic statistics for EMI survey that was conducted on a portion of the *Living Filter Field* with an EM38-MK2 meter. Other than the number of observations, all EC<sub>a</sub> values are expressed in mS/m.**

	100 EC <sub>a</sub>	50 EC <sub>a</sub>
<b>Number</b>	4302	4302
<b>Minimum</b>	-4.0	-69.9
<b>25%-tile</b>	27.7	6.5
<b>75%-tile</b>	32.5	8.4
<b>Maximum</b>	56.3	21.2
<b>Average</b>	30.1	7.3
<b>St. Dev.</b>	4.8	2.8

For the data collected with the 50-cm intercoil spacing (exploration depth of 75-cm), EC<sub>a</sub> averaged only 3.6 mS/m and ranged from -36.2 to 117.6 mS/m (Table 4). This low averaged value and the range are not considered typical of Hagerstown soil and may reflect the effects of management or meter error. The distribution of these measurements is graphed in Figure 12. As evident in this bar graph, measurements obtained with the 50-cm intercoil spacing are highly concentrated about 10 mS/m.

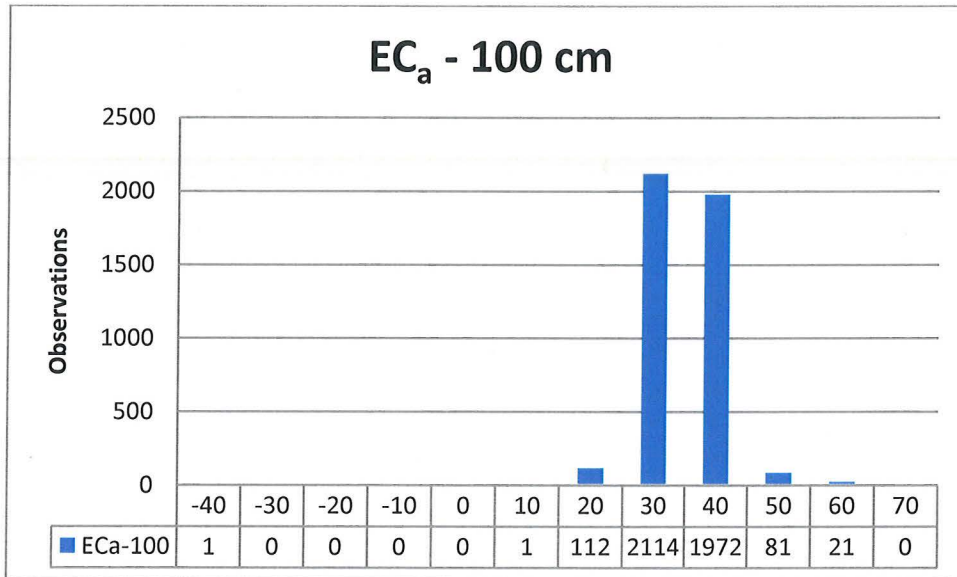


Figure 11. This bar graph shows the distribution of EC<sub>a</sub> measurements for the 0 to 150 cm depth interval.

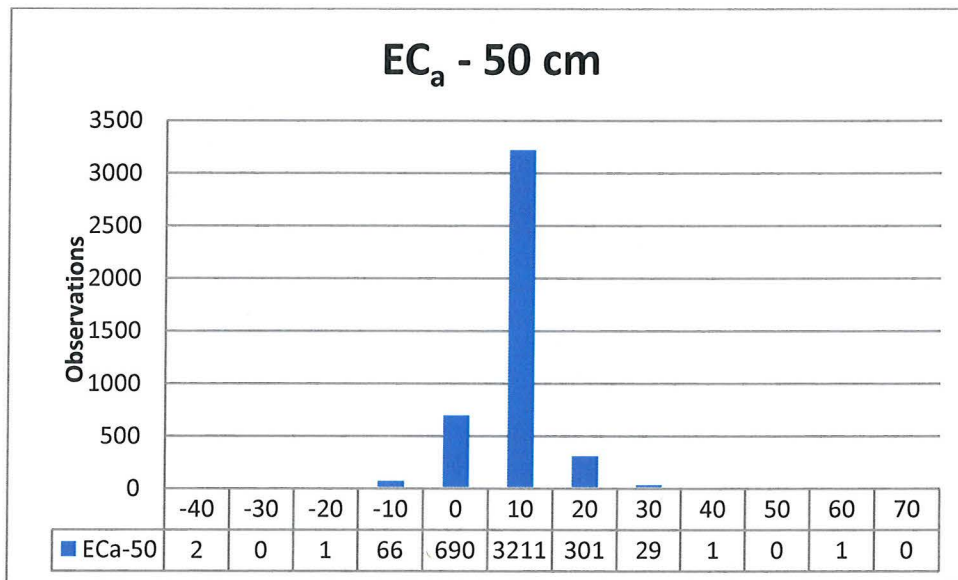


Figure 12. This bar graph shows the distribution of EC<sub>a</sub> measurements for the 0 to 75 cm depth interval.

Figure 13 contains two-dimensional (2D) plots of the EC<sub>a</sub> data collected for the shallower sensing, 50-cm (upper plot) and deeper sensing, 100-cm (lower plot) intercoil spacings. In these plots, the soil boundary lines have been imported from Web Soil Survey data<sup>5</sup>. In the plot of EC<sub>a</sub> data collected with the 100-cm intercoil spacing, higher EC<sub>a</sub> is recorded near a buried drainage line that is located in the south-central portion of this field. In both plots, areas with anomalously low or negative EC<sub>a</sub> are associated with scattered metallic debris and drainage and irrigation pipes. Comparing these two plots, it is obvious that EC<sub>a</sub> increases with increasing soil depth. This relationship is assumed to be a function of higher moisture

<sup>5</sup> Soil Survey Staff, Natural Resources Conservation Service, United States Department of Agriculture. Web Soil Survey. Available online at <http://websoilsurvey.nrcs.usda.gov/> accessed [06/4/2013].

and clay contents at lower soil depths. However, measurements made with the shallower-sensing 50-cm intercoil spacing seem to be unusually low and may reflect instrument or calibration errors.

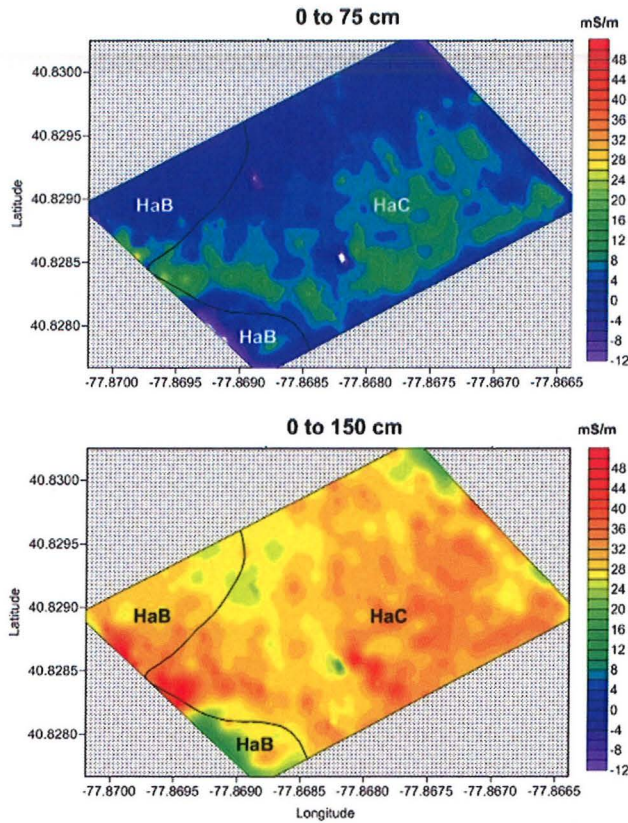


Figure 13. An EM38-MK2 meter was used to obtain these spatial  $EC_a$  measurements across the southern, cultivated portion of the *Living Filter Field*.

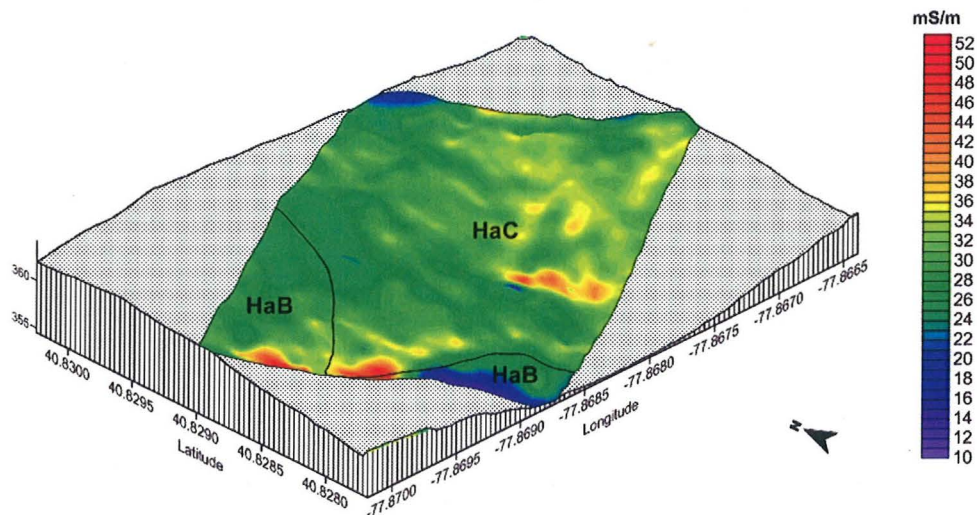


Figure 14. A two-dimensional contour plot of the  $EC_a$  measurements collected with the 100-cm intercoil spacing of an EM38-MK2 meter is overlaid on a three-dimensional wireframe image of the study site. Elevation data used to construct the wireframe image were collected with a GPS receiver.

In Figure 14, a 2D contour plot of the  $EC_a$  data collected with the 100-cm intercoil spacing of the EM38-MK2 meter has been overlain on a three-dimensional (3D) wireframe image of the *Living Filter Field* study site. Elevation data used to construct this 3D wireframe image were obtained with the Ag114 L-band DGPS antenna. In Figure 14, anomalous  $EC_a$  measurements in the south-central portion of the study site form a linear pattern that is associated with a buried drainage pipe. The sources of the anomalously low and high  $EC_a$  measured along the western border (center foreground in Figure 14) of the study area is presently unknown, but are suspected to represent a buried pipe that was passed over with the EMI meter at different distances.

**References:**

Daniels, D. J., 2004. Ground Penetrating Radar; 2<sup>nd</sup> Edition. The Institute of Electrical Engineers, London, United Kingdom.

Geonics Limited, 2007. EM38-MK2-2 ground conductivity meter operating manual. Geonics Ltd., Mississauga, Ontario.

Jol, H., 2008. Ground Penetrating Radar: Theory and Applications. Elsevier Science, Amsterdam, The Netherlands.

Merkel, E., 1978. Soil Survey of Huntingdon County, Pennsylvania. USDA-Soil Conservation Service in cooperation with Pennsylvania State University College of Agriculture and the Pennsylvania Department of Environmental Resources and State Conservation Commission. Government Printing Office, Washington DC.